BBA - Molecular Basis of Disease 1865 (2019) 2716–2725

Contents lists available at ScienceDirect

BBA - Molecular Basis of Disease

journal homepage: www.elsevier.com/locate/bbadis

Adseverin modulates morphology and invasive function of MCF7 cells

J. Tanic, Y. Wang, W. Lee, N.M. Coelho, M. Glogauer, C.A. McCulloch*

Faculty of Dentistry, University of Toronto, Canada

ARTICLE INFO

Keywords:
Actin filaments
Cell migration
Collagen degradation
Phagocytosis

ABSTRACT

Adseverin (Ads) is a Ca^{2+}-dependent actin-capping and severing protein that is highly expressed in gastric, prostate and bladder cancer cells. Currently it is unknown whether Ads contributes to the subcortical actin remodeling associated with the formation of cell extensions and matrix invasion in cancer. We compared cell extension formation and matrix degradation in Ads wildtype and Ads-null MCF7 breast cancer cells generated by CRISPR/Cas9. Compared with wildtype, Ads-null cells plated on fibronectin or collagen exhibited a more circular morphology with shorter cell extensions (37% reduction on fibronectin; $p < 0.001$). Reconstitution of Ads in Ads-null cells restored the formation of cell extensions ($p < 0.05$). While cell migration on two-dimensional matrices was unchanged by Ads deletion, the formation of cell extensions across Transwell membranes was reduced (~40% reduction, $p < 0.05$). When plated on fibrillar collagen, compared with wildtype, Ads-null cells showed reduced expression of MT1-MMP, collagen degradation ($p < 0.05$) and phagocytosis of collagen-coated beads (25% reduction; $p = 0.001$). We conclude that Ads is involved in the formation of cell extensions and collagen degradation in MCF7 cells, which may in turn affect matrix invasion and metastasis.

1. Introduction

The regulation of the assembly of subcortical actin filaments is important for the formation of cell extensions, which are involved in extracellular matrix invasion by cancer cells [1–3]. Proteases associated with cell extensions traffic to the cell surface, pass through a dense cortical actin network and upon release from the cell, degrade the pericellular matrix in local invasion processes [4,5]. The mechanisms that regulate these processes are poorly defined but there are likely a finite number of these mechanisms as cells exhibit a limited set of different motility systems for migration through extracellular matrices [6]. Importantly, cell motility and invasion rely on dynamic reorganization of the actin cytoskeleton, which enables cells to interact with the extracellular matrix and generate specialized structures that facilitate cell movement [3]. As therapeutic targeting of matrix invasion-regulating factors could decrease the morbidity associated with cancer metastasis, an improved understanding of cell extension formation and matrix degradation is important for rational development of new therapies.

Adseverin (Ads) is a member of the gelsolin family of actin binding proteins that sever and cap actin filaments [7,8]. Ads is implicated in several types of cancers, possibly through its effects on cell migration and proliferation [9,10]. Prior to the study of its potential role in cancer, Ads was examined in the context of osteoclast formation [11] and exocytosis by chromaffin cells [12]. These processes rely on the reorganization of cortical actin filaments. In chromaffin cells, Ads regulates catecholamine-containing vesicle exocytosis in response to calcium stimulation [13] while in osteoclasts Ads regulates the actin structures used by osteoclasts for bone resorption [14]. Ads binds to actin filaments in a Ca^{2+}-dependent manner and its severing activity is inhibited by membrane phospholipids. The localization of Ads and its regulators to subcortical sites suggests that Ads could play a role in modulating cortical actin to regulate cell shape [15] and potentially, cell motility.

Ads is over-expressed in a cisplatin-resistant human bladder cancer cell line (HT1376) [16] and several different gastric cancer cell lines [9,10]. In the gastric cancer cell line SGC-7901 and in PC3 cells (an invasive prostate cancer cell line), reduction of Ads expression affects proliferation and migration [9,17]. In gastric cancer cell lines that express Ads at high levels, knockdown of Ads reduces migration and invasion in vitro, tumor formation and metastasis in nude mice [10], and inhibits filopodia formation and Cdc42 expression. These data suggest a role for Ads in the formation of cell extensions in cancer cells.

We considered that Ads regulates cortical actin networks, potentially facilitating the transit of matrix-remodeling factors across the cell membrane to promote matrix degradation and the development of pro-

Abbreviations: Ads, adseverin; ECM, extracellular matrix; EMT, epithelial-mesenchymal transition; KO, knockout; TCP, tissue culture plastic; WT, wildtype

* Corresponding author at: Faculty of Dentistry, University of Toronto, 124 Edward Street, Toronto, ON M5G 1G6, Canada.
E-mail address: christopher.mcculloch@utoronto.ca (C.A. McCulloch).

https://doi.org/10.1016/j.bbadis.2019.07.015
Received 24 March 2019; Received in revised form 1 July 2019; Accepted 27 July 2019
Available online 29 July 2019

invasive cell extensions. These processes potentiate matrix invasion and cell migration. In view of the linkages of Ads with cancer [10,16,18,19], we examined the impact of Ads expression on the formation of cell extensions and pericellular matrix proteolysis. During a screen of some commonly used cell lines, we found that Ads is expressed in MCF7 cells, albeit at lower levels than PC3 cells. Accordingly, we examined how increases or reductions of Ads expression affect cancer cell behavior. Further, as breast cancers commonly metastasize to bone and in view of Ads expression in osteoclasts, which are bone-associated cells, we focused on MCF7 cells (as exemplars of breast cancer cells) and their invasive properties. We deleted Ads in MCF7 cells using CRISPR/Cas9 and examined the morphology and function of these cells in 2-dimensional and 3-dimensional cultures. Our main findings are that deletion of Ads inhibits the formation of cell extensions, cell migration across Transwell membranes and pericellular collagen degradation. As Ads is known to affect the assembly of actin filaments in osteoclasts and chromaffin cells, we suggest that Ads also regulates sub-cortical actin filaments to enable the formation of invasive structures in cancer cells.

2. Materials and methods

2.1. Reagents

Mouse monoclonal antibody to Ads (SC-376136) was from Santa Cruz Biotech (Santa Cruz, CA). Mouse monoclonal antibody to β1 integrin (12G10) and goat anti-mouse IgG antibodies were from Abcam (Cambridge, UK). Rabbit antibodies to a ¾ fragment of collagenase-cleaved type-1 collagen were purchased from Immunoglobe (Himmelstadt, Germany). Mouse monoclonal antibodies to β-actin, vinculin, and bovine plasma fibronectin were obtained from Sigma-Aldrich (St. Louis, MO). Type-1 bovine collagen (5010) was from Advanced BioMatrix (San Diego, CA). Alexa Fluor® 488 goat anti-mouse, Alexa Fluor® 568 goat anti-rabbit IgG antibodies, and rhodamine phalloidin were from Life Technologies (Burlington, ON). IL-1β, TNF-α and RANKL were purchased from R&D Systems (Minneapolis, MN).

2.2. Cells

Human PC-3 cells (CRL-1436) were purchased from American Type Culture Collection (Manassas, VA) and maintained in Dulbecco's Modified Eagle's Medium (DMEM; Wisent Bioproducts, St. Bruno, QC) supplemented with 10% fetal bovine serum (FBS) and antibiotics (164 IU/mL penicillin G, 50 μg/mL gentamicin and 0.25 μg/mL of fungizone). Human MCF7 (HTB22) cells were purchased from Wisent and maintained in modified Eagle's Medium (α-MEM; Wisent) and supplemented with 10% FBS and antibiotics. Cells were cultured at 37 °C in a humidified incubator supplied with 5% CO_2 and passaged with 0.25% trypsin containing 1 mM EDTA. For assessing Ads responses to cytokines, cells were plated overnight, grown until confluence, serum-starved and treated with IL-1β, TNF-α or RANKL for 24 h.

2.3. Ads deletion by CRISPR/Cas9

An Ads KO cell line was generated from MCF7 cells by Applied Stem Cell (Milpitas, CA) using CRISPR/Cas9 genome editing technology. Two guide RNAs (gRNAs) 5′-TATACCACGAAGAGTTCGCC-3′ and 5′-GCTC ACGGCGACTTCTACGT-3′ targeting human Ads exon 1 were chosen (Supplementary Fig. 1). The selected gRNAs were cloned into a gRNA/Cas9 expression vector and introduced to MCF7 cells. Mutagenesis within the targeted region in a single homozygous cell clone isolated from the pooled transfected cells was identified by polymerase chain reaction (PCR), using a primer pair 5′-CACTTAGCCCCTCCCGTTT CAG-3′ (forward) and 5′-CTCAGTTTGCGGTCCCCTTTACTC-3′ (reverse). Sanger sequencing (primer 5′-GTGGCGGCGAATAAGGTTCC-3′) confirmed a 92 bp (from nt 31 to 122 in the open reading frame) deletion, which led to frameshift mutation and the formation of a premature stop codon (Supplementary Fig. 2C). The deletion of Ads was confirmed at the mRNA level by reverse transcription (RT)-PCR (primers forward 5′-GGAAGCGATCGTCTCCTCTG-3′ and reverse 5′-AGCT TCTCAATCCTCCAGACC-3′ for Ads and primers forward 5′-CATGTAC GTTGCTATCCAGGC-3′ and reverse 5′-CTCCTTAATGTCACGCACGAT-3′ for β-actin) and at the protein level by immunoblotting (Supplementary Fig. 2A).

2.4. Immunoblotting

Cells were washed with ice-cold PBS and lysed in RIPA buffer (Sigma) containing phenylmethylsulfonyl fluoride, $NaVO_4$ and a protease inhibitor cocktail, and collected using a cell scraper. For all steps leading up to gel electrophoresis, procedures were performed on ice. Lysates were centrifuged at 9,600 ×*g* at 4 °C for 5 min to remove cellular debris. Total protein concentrations were determined by BCA protein assay. Samples in Laemmli sample buffer were boiled at 95 °C for 10 min and resolved by SDS-PAGE on 8–12% polyacrylamide gels containing 0.1% SDS. Electrophoresed samples were transferred to nitrocellulose membranes and blocked in 5% fat-free milk in Tris-buffered saline with Tween® 20 (TBS-T) for 1 h at room temperature. Membranes were incubated with primary antibodies in the blocking buffer overnight at 4 °C, washed with TBS-T, incubated with secondary antibodies for 1 h at room temperature and washed. The fluorescence attributable to bound antibodies was visualized and analyzed using a LI-COR Odyssey CLx. For each experimental condition, three different cultures were analyzed by immunoblotting and densitometry.

2.5. Ads rescue

Cells were transfected with Ads-EGFP as described [8]. The construct was introduced to Ads-null cells by Amaxa® Nucleofector® technology. Cells were plated on fibronectin-coated glass slides and the length of cell extensions was measured 24 h and 48 h after transfection. Empty vector pEGFP-C1 was used as the negative control.

2.6. Immunostaining and confocal microscopy

Equal numbers of cells were seeded on to glass, or fibronectin-coated glass, or fibrillar collagen gels and incubated for various times, rinsed with warm PBS, fixed in 1 or 4% paraformaldehyde (PFA) in PBS, and blocked with 1% BSA in PBS. Cells plated on glass and fibronectin were permeabilized and stained with 4′,6-diamidino-2-phenylindole (DAPI) in NP-40 (1 μg/mL), incubated with primary antibody for 1 h at 37 °C, incubated with an Alexa Fluor® 488-conjugated secondary antibody and rhodamine phalloidin or Alexa Fluor® 647 phalloidin for staining of actin filaments. Images were obtained with a Leica SP8 confocal microscope (Mannheim, Germany) at 40× or 60× objective magnification.

2.7. Cell migration and proliferation

For 2D migration, cells were plated on tissue culture plastic (TCP) and at confluence, a P200 pipet tip was used to create a scratch wound. Three different points of the scratch were marked and measured for analysis at hr 0 and hr 20 after creation of the scratch. For 3D migration, cell culture medium (600 μL containing 15% FBS) was added to each well of a 24-well plate to serve as a chemoattractant. Transwell inserts (8 μm pore size) were placed into the medium-containing wells. Equal numbers of cells (2×10^5; in 200 μL serum-free medium) were added to each insert. Cells were cultured for 24 h, fixed, stained with DAPI and rhodamine-phalloidin at 37 °C, and visualized by confocal microscopy. The number of cells and cell extensions were counted and the number of extensions formed per cell was calculated. For cell proliferation, equal numbers of cells (2×10^5/well) were plated on 6-well

plates in medium containing 10% fetal bovine serum. Cells were detached and counted every 24 h up to 4 days ($n = 3$) using a Luna-II Automated Cell Counter (Logos Biosystems, Gyeonggi-Do, South Korea).

2.8. Collagen degradation assays

Collagen gels were prepared as described [20] using bovine type I collagen (1 mg/mL; Advanced BioMatrix) on glass coverslips. Cells were incubated overnight on gels, washed, fixed with 4% PFA, and stained with rhodamine phalloidin and a neoepitope antibody that recognizes degraded type I collagen (3/4 fragment) to visualize pericellular collagen degradation. To ensure that only pericellular collagen was immunostained, cells were not permeabilized. Only the optical sections that showed cells directly in contact with the collagen gel were used for analysis of collagen degradation. For imaging, at least 30 cells each in 5 different experiments for each experimental condition were analyzed, a sample size that enabled accurate estimation of type I statistical error. For collagen degradation studies, type I collagen (1 mg/mL) was neutralized to pH 7.4 and coated on 100 mm tissue culture dishes. Cells were plated on fibrillar collagen layers for 24 h, lysed in RIPA buffer and centrifuged at 9600 $\times g$ for 10 min. Pellets and supernatants were separated on an 8% SDS-PAGE gel for immunoblot analysis of type, I collagen.

For collagen phagocytosis, cells were incubated with collagen-coated Alexa Fluor® 488 fluorescent beads (2 μm in diameter) for 2.5 h. Cell suspensions were prepared and analyzed for bead internalization by flow cytometry as described [21].

2.9. β1 integrin expression

For measurement of cell surface levels of β1 integrin, cells were cultured on TCP for 24 h, fixed but not permeabilized, stained with the 4B4 monoclonal antibody (Beckman-Coulter, Brea, CA) and analyzed by flow cytometry (BD, Franklin Lakes, New Jersey).

2.10. Statistical analysis

Mean and standard errors were computed for all continuous variables. When appropriate, two-sample comparisons were made using Student's *t*-test or the Mann-Whitney Rank sum test depending on the nature of the sample distribution. A type-1 error rate of $p < 0.05$ was set for statistical significance. All experiments were performed at least 3 times.

3. Results

3.1. Ads expression

Previous studies suggested Ads localizes to subcortical actin-rich regions of cells and our immunostaining showed prominent Ads in the sub-cortical region of PC3 and WT MCF7 cells that co-localized with actin filaments (Fig. 1A). Immunoblots showed abundant Ads expression in PC3 cells and WT MCF7 cells cultured with 10% fetal bovine serum but there was no detectable Ads in 3T3 cells (Fig. 1B). In other cancer cell lines (A549 lung cancer cells and MDa-MB-231 breast cancer), cells were analyzed for Ads protein expression (Supplementary Fig. 2B). RT-PCR analysis also showed Ads mRNA expression in WT MCF7 and PC3 cells (Fig. 1C), consistent with the immunoblot analysis. Compared with PC3 cells, MCF7 cells expressed detectable but less Ads, which was demonstrable in immunoblot and RT-PCR analysis (Fig. 1B, C). Accordingly, we restricted our focus to Ads expression in MCF7 cells because Ads is activated by RANKL in osteoclasts [22]. Further, as breast cancers commonly metastasize to bone [23], we considered that Ads might be involved in bone metastasis from breast cancer. From this rationale, we stimulated MCF7 cells with cytokines that are known to activate Ads in osteoclasts [22]. In response to IL-1β, TNF-α or RANKL, Ads expression was enhanced in WT MCF7 cells (Fig. 1D, E). Arising from these experiments, we created an MCF7 cell line in which Ads was deleted with the use of CRISPR/Cas9 (Supplementary Fig. 1). Deletion of Ads at the genomic level was evident by PCR (Fig. 1E) and deletion of Ads mRNA expression was confirmed by RT-PCR (Fig. 1F). Immunoblot analysis of the Ads-null MCF7 cells showed loss of Ads expression compared with WT MCF7 cells (Fig. 1G, Supplementary Fig. 2A). To ensure that there was no compensatory change of other gelsolin family proteins or actin regulatory proteins, we probed for gelsolin or cortactin expression and found no difference in expression levels in Ads-null cells (Fig. 1G). By flow cytometry analysis, cell surface β1 integrin expression was also unchanged in Ads-null cells compared with WT cells (Fig. 1H).

3.2. Loss of Ads promotes aggregation of MCF7 cells into discrete foci

Compared with WT cells, initial examination by phase contrast microscopy showed that when Ads-null cells were plated on tissue culture plastic (TCP) they formed clumps that were not manifested by WT cells. Accordingly, prior to re-plating, cells were counted, vigorously dispersed and visually inspected to ensure the formation of single cell suspensions. Cells were plated at equal density on TCP or fibronectin-coated glass slides and incubated for 24 h to allow for adherence and proliferation. After 24 h, WT cells were evenly distributed across cell culture plates whereas KO cells formed clumps of cells whose plasma membranes were closely approximated (Fig. 2A). We quantified this phenomenon by plating cells on glass coverslips coated with fibronectin and counted the number of DAPI-stained, attached cells in microscopic fields (fixed size of 338,500 μm^2). In WT cell cultures, most of the cells were single and isolated, (i.e. one cell per focus) whereas Ads-null cells showed much more frequent, larger clusters (i.e. with > 10 cells per focus; $p < 0.01$; Fig. 2B, C). We conducted a separate type of analysis to assess cell clustering. Cells were plated, then treated with 0.25% trypsin-EDTA, suspended in PBS and analyzed by flow cytometry for side scatter and forward scatter area as measures of cell clumping. Consistent with the microscopic method, there was a higher proportion of Ads-KO cells with larger forward scatter area larger than WT cells (36%, $p < 0.001$), suggesting that KO cells form more clusters than WT cells (Fig. 2D,E).

3.3. Cell morphology is altered by Ads deletion

We considered that since Ads is an actin filament-modulating protein, changes in Ads levels would affect actin filament abundance in cells. As current literature does not indicate which actin isoforms are modulated by Ads, we co-immunostained MCF7 cells with Ads and β-actin or Ads and γ-actin and these images were assessed for colocalization (Supplementary Fig. 3A,B). Ads preferentially co-localized with β-actin ($p < 0.05$). Both β- and γ-actin were expressed by MCF7 wild and Ads knockout cells (Supplementary Fig. C). Although rhodamine phalloidin does not distinguish between actin isoforms, this staining approach was sufficient to provide information on the localization of actin filaments, regardless of isoform type.

We assessed whether cell shape is affected by deletion of Ads and whether shape changes are associated with an invasive phenotype. Cells were plated on fibronectin-coated glass, stained with rhodamine phalloidin (Fig. 3A) and the length of cell extensions, surface area and cortical actin thickness were measured. The length of extensions was estimated by measuring the shortest distance perpendicular from the tangent of the nuclear membrane that was closest to the tip of the cell extension. WT cells exhibited longer extensions than KO cells ($p < 0.001$; Fig. 3B), and cell surface area was affected by Ads expression as WT cells exhibited larger surface area than KO cells ($p < 0.001$; Fig. 3C).

We examined the effect of Ads deletion on cortical actin filament

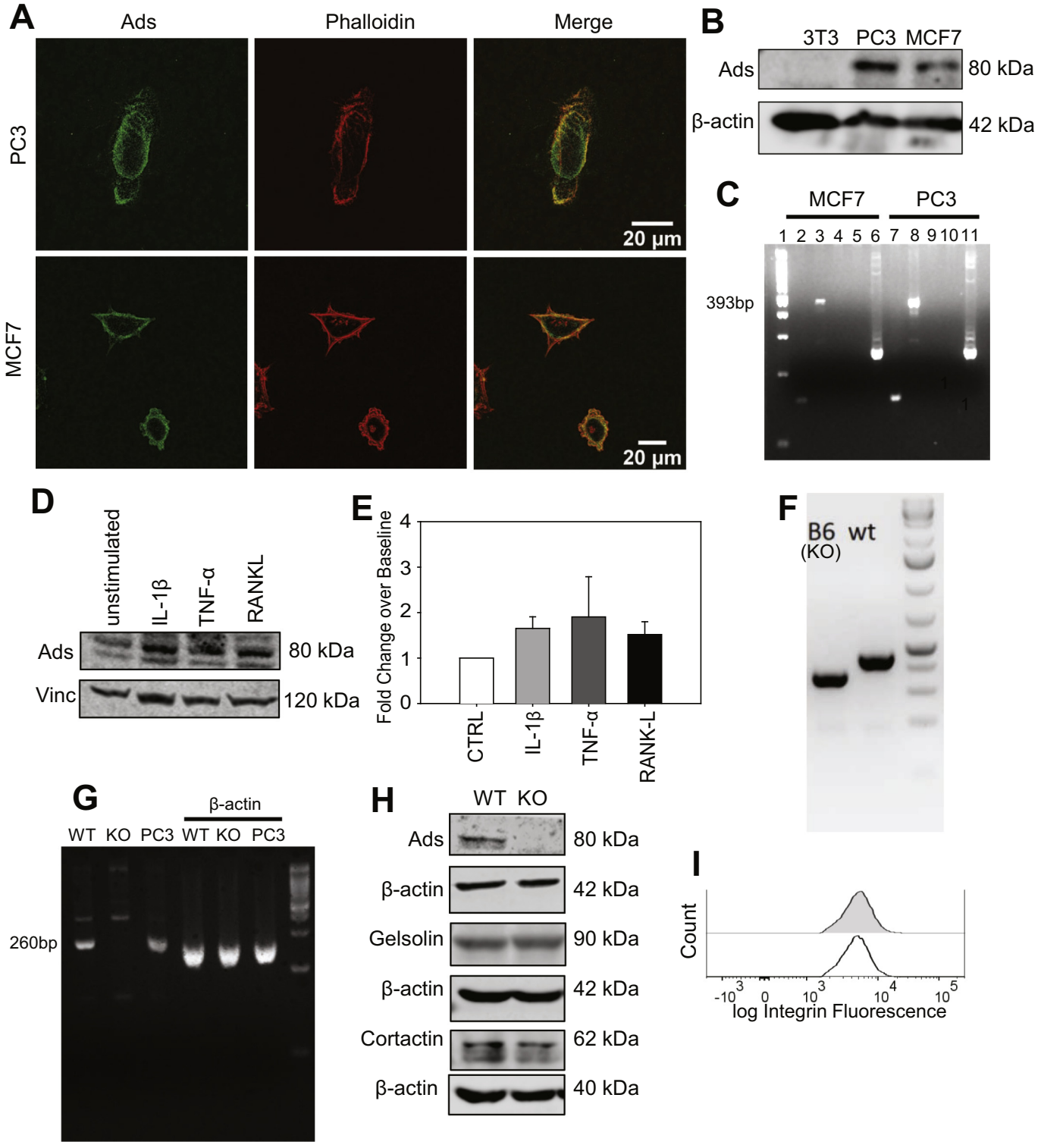

Fig. 1. Ads expression in MCF7 and PC3 cells, modulation by inflammatory cytokines and CRISPR-Cas9 deletion of Ads. (A) Immunostaining of Ads and rhodamine phalloidin staining for actin filaments in PC3 and MCF7 cells. (B) Western blot showing Ads in 3T3 cells (negative control), PC3, and MCF7 cells. (C) RT-PCR analysis of Ads mRNA in MCF7 and PC3 cells with different primer pairs. Lanes: Ladder, Primer Pair 1, (Forward: 5′- 5′-GGAAGCGATCGTCTCCTCTG-3′, Reverse: 5′-AGC TTCTCAATCCTCCAGACC-3′, Product size: 260 bp) Primer Pair 2 (Forward: 5′-GGAAGCGATCGTCTCCTCTG-3′, 2 Reverse: 5′-GAACACTCCTTTCCGAGCCA-3′, Product size: 393 bp), Primer Pair 3, Primer Pair 4, β-actin, Primer Pair 1, Primer Pair 2, Primer Pair 3, Primer Pair 4, β-actin. (D) MCF7 cells treated with pro-inflammatory cytokines and RANKL for 24 h show increased Ads expression (IL-1β - 15 ng/mL, TNF-α - 30 ng/mL, RANKL - 60 ng/mL) compared with vehicle-treated controls (unstimulated). (E) Quantification of triplicate experiments performed in blot (D). (F) PCR of genomic DNA shows deletion in cell line clone B6. Sanger sequencing (see Supplementary Fig. 2) shows a 92 base pair deletion: (GCCCGGGCGGGCAAGCAGGCGGGGCTGCAGGTCTGGAGGATTGAGAAGCTGGAGCTGGTGC CCGTGCCCCAGAGCGCTCACGGCGACTTCTA), in exon 1 of human Ads. (G) RT-PCR analysis of Ads mRNA expression in MCF7 WT, Ads-null, and PC3 cells (positive control). Lanes 1–3: primers directed to Ads exon 1, Lanes 4–6: β-actin control, Lane 7: ladder. (H) Immunoblot of Ads, gelsolin, and the cell extension-associated protein, cortactin. (I) Flow cytometry shows no shift of fluorescence intensity after staining with 4B4 antibody, which binds to β1-integrin, a fibrillar collagen receptor. Ads WT (gray peak); KO cells (white peak).

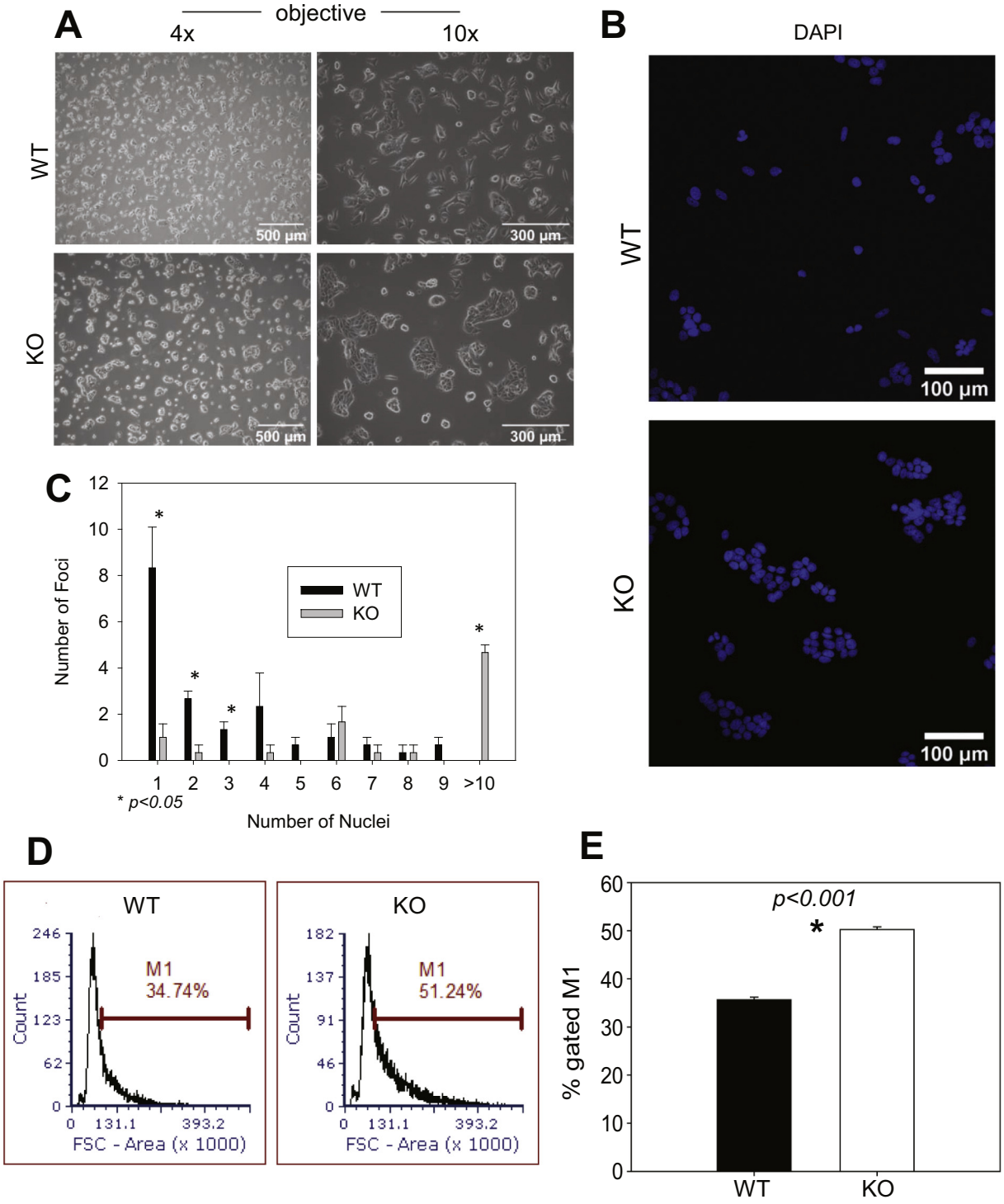

Fig. 2. Ads knockout promotes cell clustering. (A) WT or KO cells plated for > 24 h on tissue culture plastic at low (4×) and higher magnification (10×) objectives. (B) WT and KO cells plated on fibronectin-coated glass and stained with DAPI. (C) Quantification of number of nuclei per group of cells whose cell membranes are in direct physical contact (defined here as a focus). WT cells exhibit higher numbers of single, isolated cells after culture (1 cell/focus) compared with KO cells, which show larger clusters (> 10 cells/focus). (D) Flow cytometry shows size-shift (i.e. to the right side of the histogram) in the proportion of Ads-KO (right) cells. Note the larger forward scatter area (gate M1) compared with WT cells (left). (E) Quantification of cells in the M1 gate.

remodeling by quantifying the fluorescence intensity of the cortical actin network and dividing this datum by the surface area of the actin filament region of interest (ROI) to adjust for differences in the surface area selected for analysis. The cortical actin network was defined as the zone of actin filaments directly subjacent to the plasma membrane that directionally tracked with the trajectory of the plasma membrane. Deletion of Ads resulted in higher phalloidin fluorescence per unit area of the cortical actin network ($p < 0.05$; Fig. 3D), indicating that there were more abundant actin filaments in the cortex of KO cells. For examining the effects of restoration of Ads expression on the formation of cell extensions, Ads-EGFP construct was transfected into Ads-null cells. Transfection of cells with mouse Ads-EGFP restored the formation of

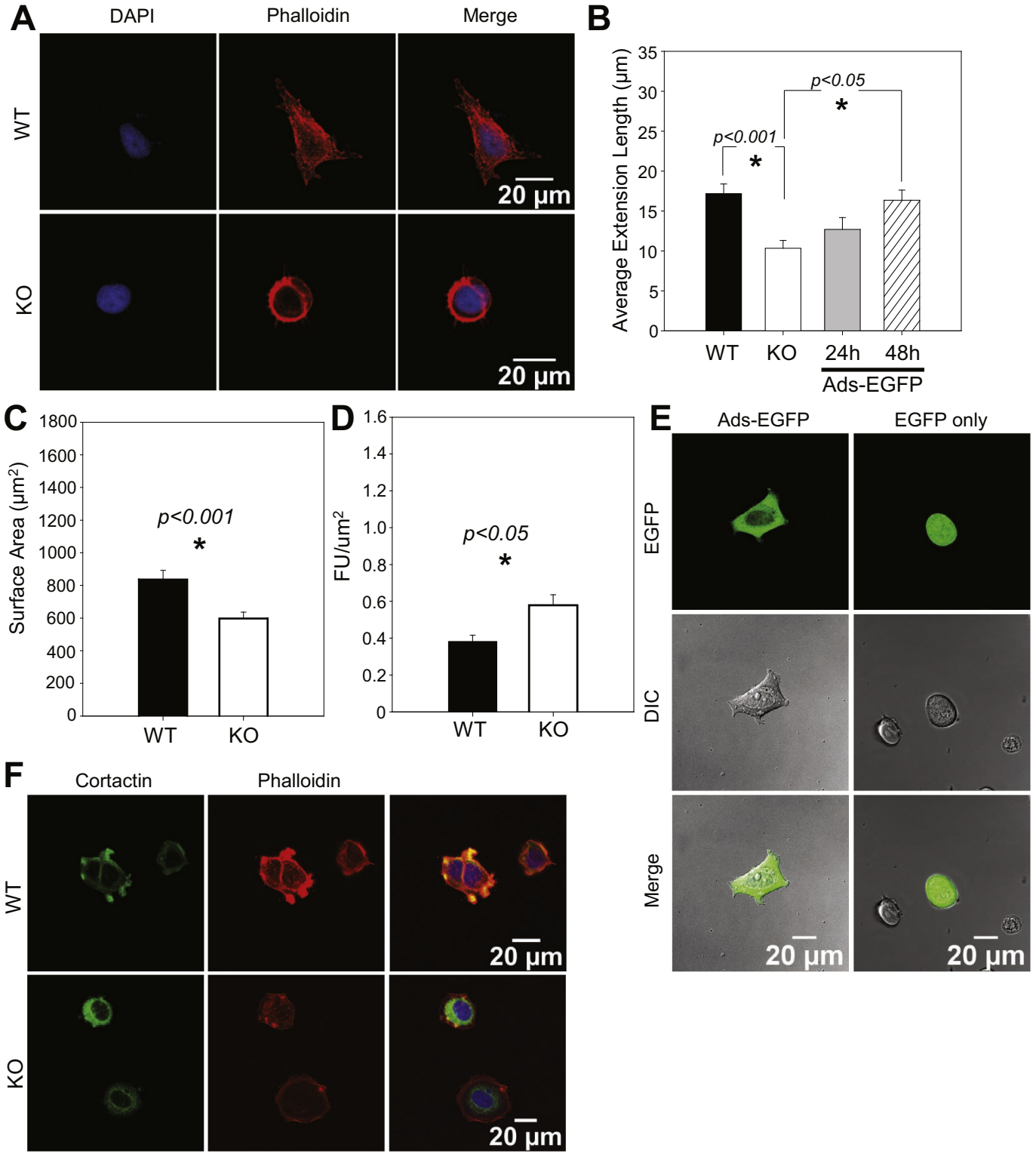

Fig. 3. Ads knockout affects cell morphology, cell extensions and sub-cortical actin. (A) Actin filaments in Ads-WT and KO MCF7 cells that were plated on fibronectin. Nuclei (DAPI) are stained in blue; actin filaments (phalloidin) are stained in red. (B) KO cells exhibited shorter cell extensions (measured from the edge of the cell nucleus) than WT cells ($p < 0.001$). Re-expression of Ads in Ads KO cells at 48 h after Ads-EGFP transfection restores cell extension formation ($p < 0.05$). (C) KO cells exhibit reduced surface area compared with WT cells ($p < 0.001$). (D) Abundance of cortical actin filaments (FU/µm^2) is higher ($p < 0.05$) in KO cells compared with WT cells. (E) Reconstitution of Ads expression in KO cells restores extension formation. (F) Immunostaining for cortactin (green) and affinity labeling of actin filaments (phalloidin; red) in WT and KO cells.

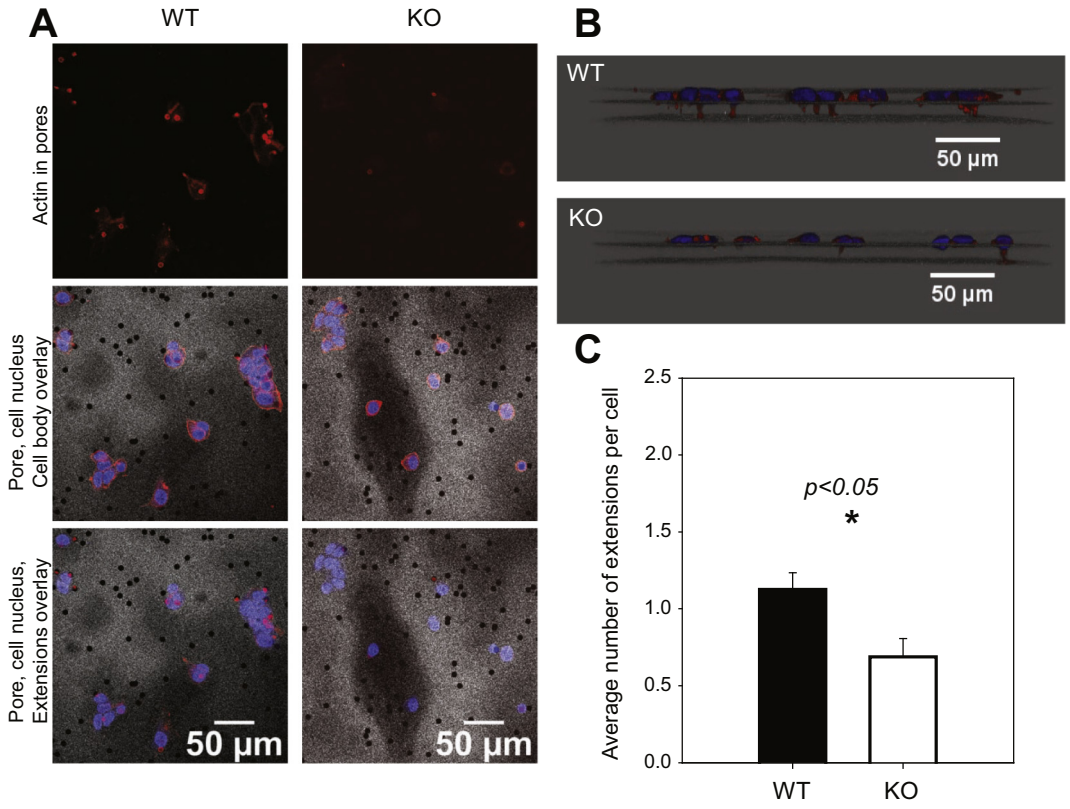

Fig. 4. Ads knockout reduces cell extension formation in 3D cultures. (A) Images of previously serum-starved WT or KO cells plated on 8 µm pore-size Transwell membranes using 15% fetal bovine serum as a chemoattractant in the lower part of the wells. Cells were fixed and imaged 24 h after plating. (B) Y-Z axes side-view image of cell extension formation in WT and Ads-null cells migrating across Transwell membranes. DAPI (blue), rhodamine phalloidin (red). (C) Quantification of number of extensions formed per cell across Transwell membrane in Ads WT and KO cells ($p = 0.015$).

cell extensions (Fig. 3B), suggesting that Ads mediates cell extension formation in MCF7 cells. Notably, while Ads deletion did not affect total levels of cortactin expression (Fig. 1G), cortactin was redistributed from the tips of cell extensions in WT cells to a predominantly perinuclear location in Ads-null cells (Fig. 3F).

3.4. Effect of Ads on cell migration

As cell motility is dependent in part on the ability of cells to form actin-rich protrusive structures, the effect of Ads expression on cell shape and subcortical actin filament density shown above suggested that Ads may impact cell migration. Accordingly, to assess the effect of Ads on cell migration, cells were examined in Transwell migration assays. Cell extensions that extended through the 8 µm diameter pores of the Transwell membrane were quantified. A serum gradient was created to promote cell migration across the membrane and actin filaments stained with phalloidin were visualized by confocal microscopy (Fig. 4A). The number of cell extensions in the pores of the Transwell membrane was used as a measure of migration as cells form invasive structures that migrate across the membrane. Only cells that were positioned on top of a pore or were adjacent to a pore (so that they would be able to extend a process down the pore) were quantified. DAPI-stained nuclei were used to identify individual cells and the cell bodies with which they were associated to quantify cell numbers. WT cells generated 1.6-fold more extensions than Ads-null cells ($p < 0.05$; Fig. 4B,C), indicating that of Ads expression enhances the formation of 3D migratory structures. Notably, deletion of Ads did not affect cell proliferation (Supplementary Fig. 4) and in response to a scratch wound on two-dimensional TCP surfaces (Supplementary Fig. 5A,B), there was no difference between the ability of WT and Ads-null cells to migrate into the cell-denuded area ($p = 0.79$; Supplementary Fig. 4C).

3.5. Ads enhances collagen degradation and internalization

The Ads-dependent promotion of a morphology consistent with 3D migration suggested that Ads may be involved in facilitating invasion through the collagen matrix. Accordingly, cells were plated on fibrillar collagen gels for 24 h and fixed but not permeabilized to ensure that the collagen degradation assessed by immunostaining (antibody recognition of a collagenase-generated, ¾ length degradation neo-epitope in collagen fibrils) was only extracellular and not intracellular (Fig. 5A). Images of degraded collagen were projected in the z-axis and each cell-associated ¾-collagen particle was counted in the region of interest containing the cell only. Ads null cells showed fewer numbers of labeled particles exhibiting pericellular collagen degradation ($p < 0.05$) compared with WT cells (Fig. 5B). Notably, while the morphology of WT and KO cells plated on collagen was similar to cells that were plated on fibronectin (Fig. 3A), when plated on collagen substrates, WT cells exhibited less rounding than KO cells, which had smaller surface areas (Fig. 5C). When we divided the total number of collagen degradation particles by the surface area of the cells, the mean numbers of particles were still higher in WT cells but the size of the statistical difference ($p < 0.06$; Fig. 5D) was reduced.

We considered that the Ads-associated reduction in collagen degradation could be linked to inhibition of collagen phagocytosis, a mechanism that is facilitated by pericellular matrix proteolysis [24]. To examine this link, flow cytometry to examine collagen phagocytosis [21], Ads KO cells internalized significantly less collagen-coated beads than WT MCF7 cells (25% reduction; $p < 0.001$; Fig. 5E,F).

As previous data showed that internalization of collagen is dependent on expression of MT1-MMP [24], we examined MT1-MMP in WT MCF7 and Ads-null cells. Deletion of Ads was associated with a marked reduction of MT1-MMP immunostaining in the Ads-null cells compared

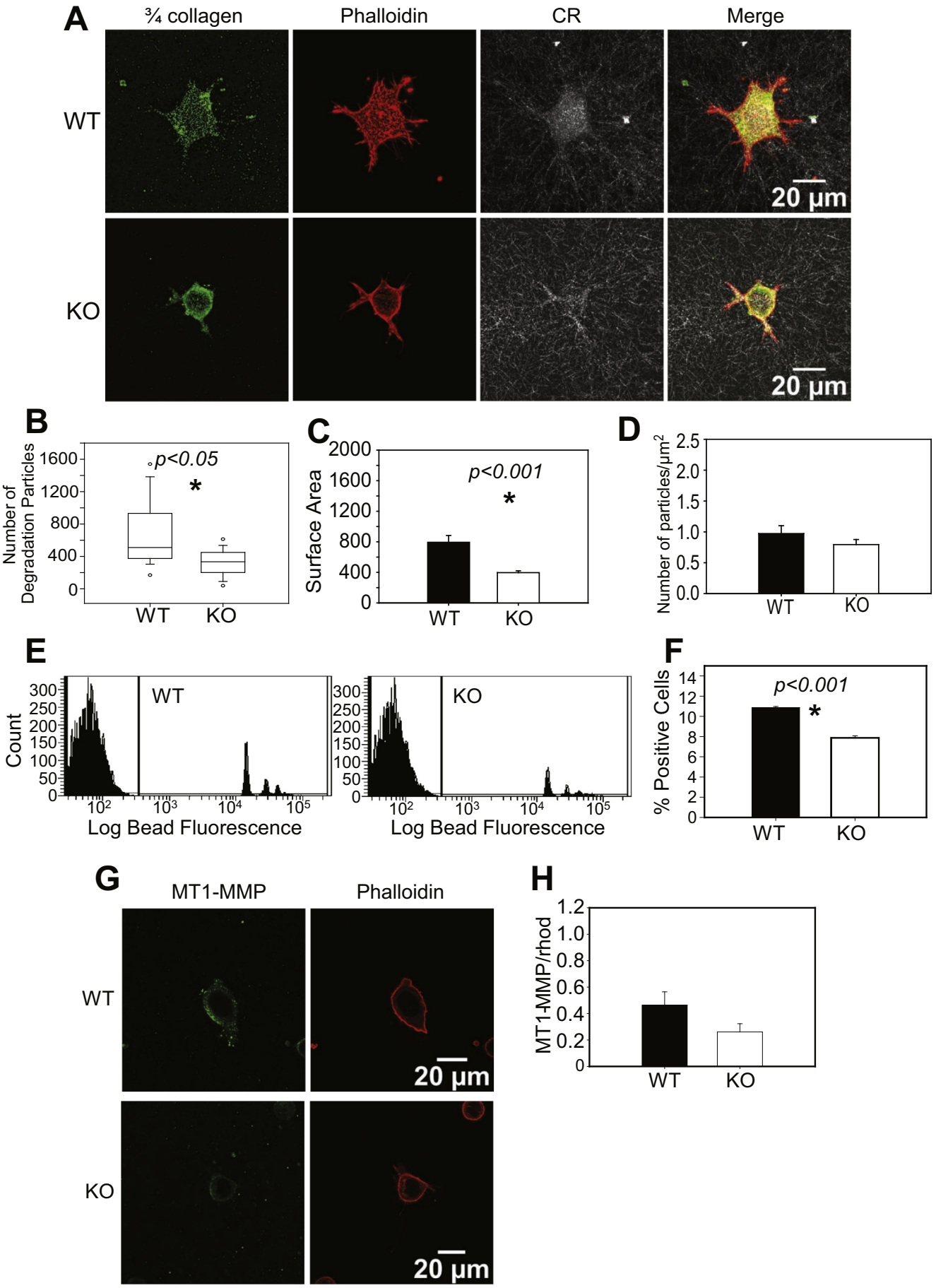

(caption on next page)

Fig. 5. Ads knockout is associated with inhibition of collagen degradation and phagocytosis. (A) Staining for ¾ collagen fragments (green), actin filaments (phalloidin; red) and intact collagen fibrils (gray) by confocal reflectance (CR) in Ads WT MCF-7 cells plated on 3D, type I collagen gels. (B) Quantification of collagen degradation stained with a ¾ collagen neoepitope antibody in WT and Ads KO cells. WT cells exhibit more collagen degradation (500–600 labeled particles/cell) compared with KO cells (~200 particles/cell), indicating that Ads is important for collagen degradation. (C) Quantification of surface area of WT and Ads KO cells plated on fibrillar collagen. (D) Quantification of number of collagen degradation particles divided by surface area of cells in WT (0.973 particles/μm^2) compared with Ads-KO cells (0.794 particles/μm^2). (E) Flow cytometry histograms depicting internalization of 2 μm diameter Alexa Fluor® 488-conjugated collagen-coated beads in Ads WT and KO cells after incubation with beads for 2.5 h. (F) Quantification of cells containing internalized beads that are shown in panel D. (G) Immunostaining of MT1-MMP in MCF7 WT and Ads-KO cells. (H) Quantification of fluorescence intensity of MT-1MMP staining normalized to actin filament fluorescence intensity (rhod).

with WT MCF7 cells ($p < 0.05$; Fig. 5G). In view of these findings, we considered whether Ads-related changes in cell shape and function might be a result of epithelial-mesenchymal transition. Accordingly, we plated cells on collagen-coated tissue culture plastic for 24 h or 72 h to enhance potential transition and analyzed vimentin, N-cadherin, and E-cadherin expression. WT MCF7 and Ads-null cells did not express detectable vimentin or N-cadherin but did express E-cadherin, suggesting that Ads does not affect expression of genes involved in epithelial-mesenchymal transition (Supplementary Fig. 5).

4. Discussion

In cancer cells, pro-invasive, actin-based structures that affect cell morphology are important for metastasis [25–27]. The actin capping and severing protein Ads is implicated in gastric, prostate, head and neck, and breast cancers [9,10,17,28] but there are limited data on the relationship between Ads expression and the invasive phenotype. As Ads severing activity alters the structure of the actin network and changes in cell shape, an improved understanding of how Ads is involved in cell function could provide better insights into the invasive functions of cancer cells. We found that in MCF7 cells, a breast cancer epithelial cell line, Ads is critical for the generation of cortactin and MT1-MMP-enriched cell extensions, which are associated with invasion of the pericellular collagen matrix. Deletion of Ads increased the density of sub-cortical actin filaments and cell rounding, but decreased cell extension length, cell migration and degradation of pericellular collagen. These data directly implicate Ads in early steps of matrix invasion.

Ads expression levels are associated with variations of proliferation and apoptosis in cultured cells [17,29]. We found that Ads expression is also related to the type of cell migration in metastatic processes. As found in 3D cell migration assays, cells expressing Ads readily generated large numbers of protrusive structures that enhance cell migration. Accordingly, to identify factors that may influence Ads expression, we stimulated MCF7 cells with IL-1β, TNF-α or RANKL. This approach was based on recent findings showing that these cytokines increase Ads in monocytes [29] and that cancer cells modify their gene expression repertoire in response to soluble immune signals [30]. We found that Ads expression was increased by these inflammatory cytokines, which underlines the notion that enhanced Ads expression in cancer cells is associated with the invasive phenotype, and might also underlie the enhanced metastasis of breast cancer cells to bone, since Ads is highly expressed in bone-associated osteoclasts. Further, as epithelial cells tend to maintain their intercellular adhesions during collective cell migration [31], our finding that cell clustering was reduced in cells expressing Ads suggests that Ads enhances single cell migration.

The impact of Ads expression on cell morphology is emphasized by the longer cell extensions, increased cell surface area and reduced abundance of cortical actin filaments in cells expressing Ads. As Ads is an actin filament-severing protein, the reduced abundance of sub-cortical actin in Ads-expressing cells was anticipated and is consistent with the ability of these cells to more efficiently generate actin-enriched structures needed for migration. The recovery of cell extensions in Ads null cells after re-expression of Ads indicates that the formation of these extensions is an Ads-mediated phenomenon and not an artefact of CRISPR/Cas9 gene editing. Further, Ads-null cells formed fewer cell extensions in 3D migration, consistent with previous reports suggesting that Ads expression is associated with increased metastasis [10,17].

Deletion of Ads affected MCF7 cell migration in a 3D but not a 2D assay system. In this context, compared with Ads-null cells, WT cells more efficiently degraded collagen, as shown by increased collagen internalization, expression of MT1-MMP and generation of ¾ collagen fragments. As Ads does not affect 2D (sheet type) cell migration, our data suggest that Ads, through its effect on pericellular matrix proteolysis, affects ECM degradation to promote invasion. It is currently unclear whether Ads enhances remodeling of cortical actin networks to facilitate exocytosis and release of matrix-degrading enzymes as well as the acceleration of actin filament growth for promoting the formation of matrix-invading structures.

A hallmark of cancer migration is the degradation and remodeling of the surrounding extracellular matrix to create sufficiently large pores in the matrix to facilitate cell migration [30]. Our data on Ads and its impact on the structure and function of MCF7 cells suggest a process by which cancer cells form actin-rich, matrix proteolytic structures. These structures facilitate remodeling of the extracellular matrix by enhancing by pericellular collagen proteolysis and phagocytosis. Data from the current study provides new insights on the functional relationship between Ads expression and cancer cell-associated matrix invasion. Accordingly, Ads may have an important role in modulating the formation of pro-invasive structures, which could be therapeutically targeted to regulate metastasis.

CRediT authorship contribution statement

J. Tanic: Conceptualization, Data curation, Formal analysis, Methodology, Validation, Visualization, Writing - original draft, Writing - review & editing. **Y. Wang:** Formal analysis, Investigation, Methodology, Validation, Visualization, Writing - original draft. **W. Lee:** Data curation, Formal analysis, Funding acquisition, Investigation, Methodology, Resources. **N.M. Coelho:** Data curation, Formal analysis, Investigation, Methodology, Validation, Visualization, Writing - review & editing. **M. Glogauer:** Conceptualization, Funding acquisition, Investigation, Methodology, Project administration, Supervision, Validation, Visualization, Writing - original draft. **C.A. McCulloch:** Conceptualization, Funding acquisition, Investigation, Methodology, Project administration, Resources, Software, Supervision, Validation, Visualization, Writing - original draft, Writing - review & editing.

Transparency document

The Transparency document associated with this article can be found, in online version.

Acknowledgements

This study was supported by a Canadian Institutes of Health Research (CIHR) grant (MOP-142250) to MG and CAM, who is supported by a Canada Research Chair (Tier 1).

Disclosure of Competing Interest

The authors declare no conflicts of interest.

Appendix A. Supplementary data

Supplementary data to this article can be found online at https://doi.org/10.1016/j.bbadis.2019.07.015.

References

[1] M. Schoumacher, R.D. Goldman, D. Louvard, et al., Actin, microtubules, and vimentin intermediate filaments cooperate for elongation of invadopodia, J. Cell Biol. 189 (3) (2010) 541–556.
[2] E. Sahai, Mechanisms of cancer cell invasion, Curr. Opin. Genet. Dev. 15 (1) (2005) 87–96.
[3] H. Yamaguchi, J. Condeelis, Regulation of the actin cytoskeleton in cancer cell migration and invasion, Biochim. Biophys. Acta 1773 (5) (2007) 642–652.
[4] E.S. Clark, A.S. Whigham, W.G. Yarbrough, et al., Cortactin is an essential regulator of matrix metalloproteinase secretion and extracellular matrix degradation in invadopodia, Cancer Res. 67 (9) (2007) 4227–4235.
[5] D. Hoshino, K.C. Kirkbride, K. Costello, et al., Exosome secretion is enhanced by invadopodia and drives invasive behavior, Cell Rep. 5 (5) (2013) 1159–1168.
[6] A.G. Clark, D.M. Vignjevic, Modes of cancer cell invasion and the role of the microenvironment, Curr. Opin. Cell Biol. 36 (2015) 13–22.
[7] J.M. Trifaro, M.L. Vitale, A. Rodriguez Del Castillo, Scinderin and chromaffin cell actin network dynamics during neurotransmitter release, J. Physiol. Paris 87 (2) (1993) 89–106.
[8] S. Hassanpour, H. Jiang, Y. Wang, et al., The actin binding protein adseverin regulates osteoclastogenesis, PLoS One 9 (9) (2014) e109078.
[9] X.M. Chen, J.M. Guo, P. Chen, et al., Suppression of scinderin modulates epithelial-mesenchymal transition markers in highly metastatic gastric cancer cell line SGC7901, Mol. Med. Rep. 10 (5) (2014) 2327–2333.
[10] J.J. Liu, J.Y. Liu, J. Chen, et al., Scinderin promotes the invasion and metastasis of gastric cancer cells and predicts the outcome of patients, Cancer Lett. 376 (1) (2016) 110–117.
[11] M.K. Song, Z.H. Lee, H.H. Kim, Adseverin mediates RANKL-induced osteoclastogenesis by regulating NFATc1, Exp. Mol. Med. 47 (2015) e199.
[12] M.G. Marcu, L. Zhang, K. Nau-Staudt, et al., Recombinant scinderin, an F-actin severing protein, increases calcium-induced release of serotonin from permeabilized platelets, an effect blocked by two scinderin-derived actin-binding peptides and phosphatidylinositol 4,5-bisphosphate, Blood 87 (1) (1996) 20–24.
[13] T. Dumitrescu Pene, S.D. Rose, T. Lejen, et al., Expression of various scinderin domains in chromaffin cells indicates that this protein acts as a molecular switch in the control of actin filament dynamics and exocytosis, J. Neurochem. 92 (4) (2005) 780–789.
[14] H. Jiang, Y. Wang, A. Viniegra, et al., Adseverin plays a role in osteoclast differentiation and periodontal disease-mediated bone loss, FASEB J. 29 (6) (2015) 2281–2291.
[15] J. Trifaro, S.D. Rose, T. Lejen, et al., Two pathways control chromaffin cell cortical F-actin dynamics during exocytosis, Biochimie 82 (4) (2000) 339–352.
[16] N. Miura, N. Takemori, T. Kikugawa, et al., Adseverin: a novel cisplatin-resistant marker in the human bladder cancer cell line HT1376 identified by quantitative proteomic analysis, Mol. Oncol. 6 (3) (2012) 311–322.
[17] D. Wang, S.Q. Sun, Y.H. Yu, et al., Suppression of SCIN inhibits human prostate cancer cell proliferation and induces G0/G1 phase arrest, Int. J. Oncol. 44 (1) (2014) 161–166.
[18] H. Liu, D. Shi, T. Liu, et al., Lentivirus-mediated silencing of SCIN inhibits proliferation of human lung carcinoma cells, Gene 554 (1) (2015) 32–39.
[19] X. Lai, W. Su, H. Zhao, et al., Loss of scinderin decreased expression of epidermal growth factor receptor and promoted apoptosis of castration-resistant prostate cancer cells, FEBS Open Bio 8 (5) (2018) 743–750.
[20] N.M. Coelho, P.D. Arora, S. van Putten, et al., Discoidin domain receptor 1 mediates myosin-dependent collagen contraction, Cell Rep. 18 (7) (2017) 1774–1790.
[21] W. Lee, J. Sodek, C.A. McCulloch, Role of integrins in regulation of collagen phagocytosis by human fibroblasts, J. Cell. Physiol. 168 (3) (1996) 695–704.
[22] Y. Wang, M. Galli, A. Shade Silver, et al., IL1beta and TNFalpha promote RANKL-dependent adseverin expression and osteoclastogenesis, J. Cell Sci. 131 (11) (2018).
[23] L. Kiesel, A. Kohl, Role of the RANK/RANKL pathway in breast cancer, Maturitas 86 (2016) 10–16.
[24] H. Lee, C.M. Overall, C.A. McCulloch, et al., A critical role for the membrane-type 1 matrix metalloproteinase in collagen phagocytosis, Mol. Biol. Cell 17 (11) (2006) 4812–4826.
[25] M.A. Eckert, T.M. Lwin, A.T. Chang, et al., Twist1-induced invadopodia formation promotes tumor metastasis, Cancer Cell 19 (3) (2011) 372–386.
[26] D.A. Murphy, S.A. Courtneidge, The ins and outs of podosomes and invadopodia: characteristics, formation and function, Nat. Rev. Mol. Cell Biol. 12 (2011) 413.
[27] H.S. Leong, A.E. Robertson, K. Stoletov, et al., Invadopodia are required for cancer cell extravasation and are a therapeutic target for metastasis, Cell Rep. 8 (5) (2014) 1558–1570.
[28] M. Hasmim, C. Badoual, P. Vielh, et al., Expression of EPHRIN-A1, SCINDERIN and MHC class I molecules in head and neck cancers and relationship with the prognostic value of intratumoral CD8+ T cells, BMC Cancer 13 (2013) 592.
[29] W. Jian, X. Zhang, J. Wang, et al., Scinderin-knockdown inhibits proliferation and promotes apoptosis in human breast carcinoma cells, Oncol. Lett. 16 (3) (2018) 3207–3214.
[30] D. Hanahan, R.A. Weinberg, Hallmarks of cancer: the next generation, Cell 144 (5) (2011) 646–674.
[31] M.S. Balda, K. Matter, Epithelial cell adhesion and the regulation of gene expression, Trends Cell Biol. 13 (6) (2003) 310–318.